Supporting Information

Zhang et al. 10.1073/pnas.1202194109

SI Discussion

Although carbachol activated the M1 receptor/Gq/PLC pathway, leading to the hydrolysis of $PI(4,5)P_2$ and activation of TRPC6, it failed to stimulate TRPML1 activity. In contrast, the breakdown of $PI(4,5)P_2$ by direct activation of 5-phosphatase was sufficient to activate TRPML1. One potential explanation for this discrepancy is that the affinity of ion channels determines their sensitivity to $PI(4,5)P_2$ (1). The insensitivity of TRPML1 to M1 receptor activation might reflect the channel's high affinity to $PI(4,5)P_2$ (IC_{50} = 0.2 μM). Although we observed a rapid carbachol-induced translocation of GFP-PLCδ1-PH, a commonly used $PI(4,5)P_2$ probe with a K_d of 1.7 μM (2), it remains unknown whether M1 receptor activation could sufficiently deplete the $PI(4,5)P_2$ level to modulate TRPML1. Moreover, activation of TRPML1 by GTP-γ-S, but not M1 receptor activation, could potentially be explained by a "receptor-specific phosphoinositide signaling" theory that highlights the importance of a local $PI(4,5)P_2$ pool in regulating the channels only adjacent to the receptors (3). Finally, the insensitivity of TRPML1 to M1 receptor/PLC activation could also be explained by the fact that receptor stimulation might activate other signaling pathways such as diacylglycerol, inositol triphosphate, Ca^{2+}, and PKC, concurrently to nullify the effect of $PI(4,5)P_2$ depletion on TRPML1 activation.

1. Suh BC, Hille B (2008) PIP2 is a necessary cofactor for ion channel function: How and why? *Annu Rev Biophys* 37:175–195.
2. Lemmon MA, Ferguson KM, O'Brien R, Sigler PB, Schlessinger J (1995) Specific and high-affinity binding of inositol phosphates to an isolated pleckstrin homology domain. *Proc Natl Acad Sci USA* 92:10472–10476.
3. Gamper N, Shapiro MS (2007) Regulation of ion transport proteins by membrane phosphoinositides. *Nat Rev Neurosci* 8:921–934.

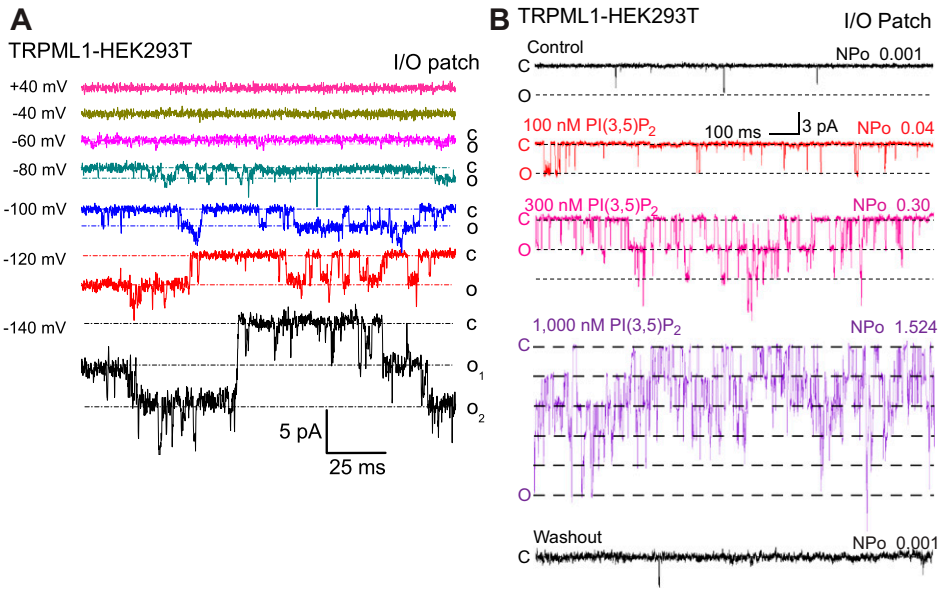

Fig. S1. Single-channel currents in an I/O patch excised from a TRPML1-expressing HEK293T cell. (*A*) Single-channel openings were elicited using a voltage step protocol from −140 mV to +80 mV (HP = 0 mV). At negative, but not positive potentials, channel openings were frequently observed. C, closed state; O, open state. (*B*) $PI(3,5)P_2$ activates single channel TRPML1 currents at the plasma membrane (PM) in a dose-dependent manner. The $PI(3,5)P_2$ effect was examined in an I/O patch excised from TRPML1-GFP–expressing HEK293T cells.

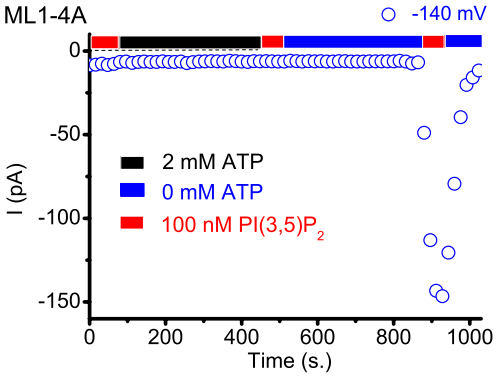

Fig. S2. Mg-ATP prevents run-up of TRPML1 currents in I/O patches. In an I/O patch, bath application of 2 mM Mg-ATP for 6 min prevented run-up of ML1-4A. Upon removal of Mg-ATP for 6 min, $I_{ML1\text{-}4A}$ was activated by 100 nM PI(3,5)P_2.

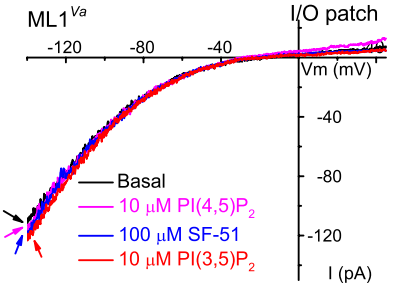

Fig. S3. Insensitivity of TRPML1^{Va} to PI(4,5)P_2. Large basal $I_{ML1\text{-}Va}$ was detected in an I/O patch excised from ML1^{Va}-expressing cells. PI(4,5)P_2 (10 μM) failed to inhibit $I_{ML1\text{-}Va}$.

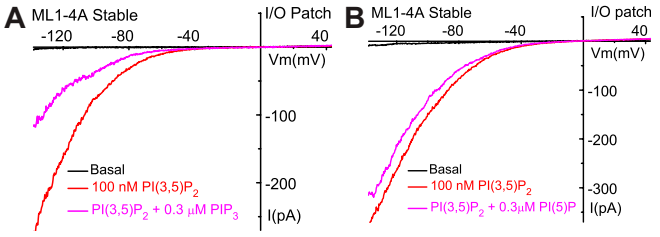

Fig. S4. Effects of PI(3,4,5)P_3 and PI(5)P on $I_{ML1\text{-}4A}$. (*A*) Inhibition PI(3,5)P_2-activated $I_{ML1\text{-}4A}$ by 300 nM PI(3,4,5)P_3 in an I/O patch excised from ML1-4A stable cells. (*B*) Lack of an effect of PI(5)P (300 nM) on PI(3,5)P_2-activated $I_{ML1\text{-}4A}$.

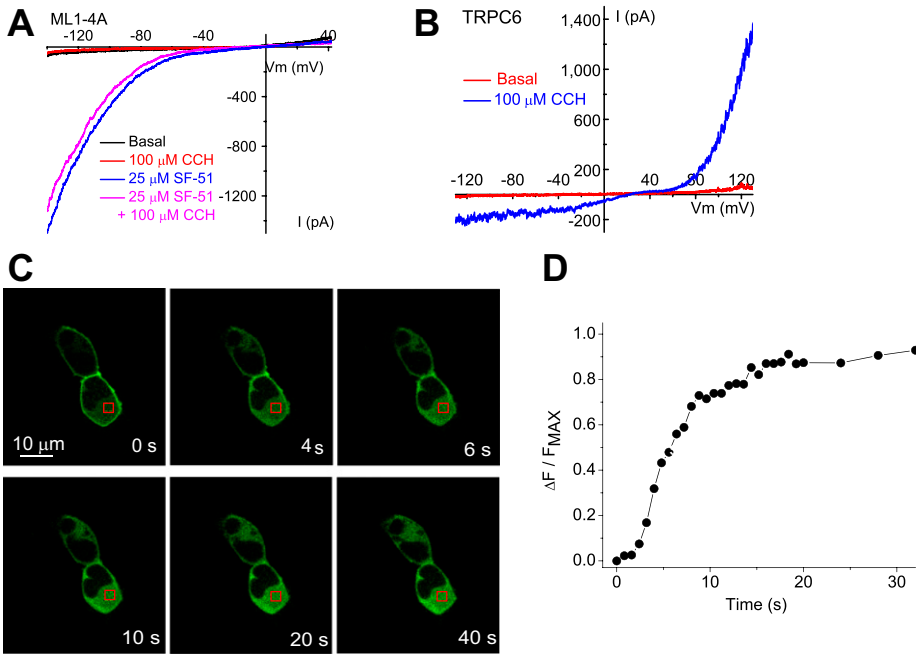

Fig. S5. Receptor-mediated activation of PLC induces $PI(4,5)P_2$ hydrolysis but fails to activate TRPML1. (*A*) Activation of PLC-coupled M1 receptors had no effect on $I_{ML1\text{-}4A}$. Carbachol (CCH; 100 μM) was used to activate the Gq/PLC pathway in HM1 cells. (*B*) Whole-cell TRPC6 currents were activated by CCH (100 μM). (*C* and *D*) CCH-induced hydrolysis of $PI(4,5)P_2$ detected using a $PI(4,5)P_2$ probe. (C) CCH (100 μM) induced a translocation of GFP–PLCδ1-PH from the plasma membrane to the cytosol. Images shown were taken 0, 4, 6, 10, 20, and 40 s after CCH application. Red boxes indicate cytosolic regions where fluorescence intensity (F) was measured. (*D*) Time course of GFP–PLCδ1-PH translocation. Changes in average fluorescence intensity ($\Delta F = F - F_{basal}$) are normalized to maximum change of fluorescence intensity (F_{max}) and plotted with time. Data were analyzed with ImageJ software (National Institutes of Health).

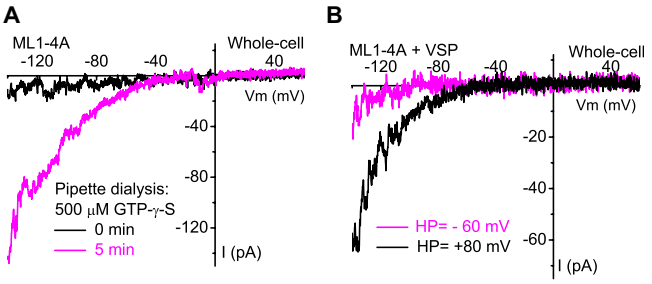

Fig. S6. GTP-γ-S and depolarization-activated Ci-VSP evoke whole-cell TRPML1 currents. (*A*) In an HM1 cell overexpressing TRPML1-4A, small whole-cell $I_{ML1\text{-}4A}$ developed gradually upon pipette dialysis of GTP-γ-S (500 μM) for 5 min. (*B*) Depolarization-activated Ci-VSP increases basal $I_{ML1\text{-}4A}$. Representative traces of whole-cell currents in Ci-VSP–transfected ML1–4A stable cells before (HP = –60 mV) and 8 min after depolarization (HP = +80 mV). $I_{ML1\text{-}4A}$ was elicited by voltage ramps (from –140 mV to +100 mV; 100-ms duration).

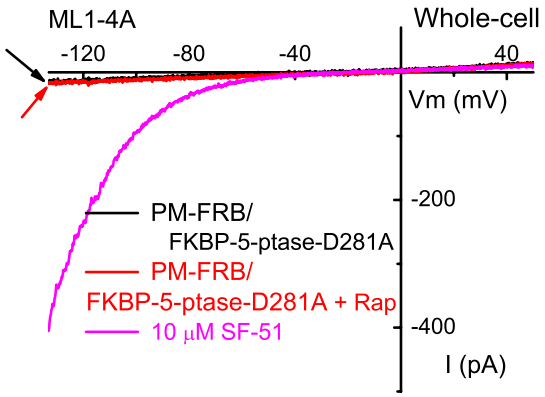

Fig. S7. PM-translocation of inactive mutant FKBP-5-phosphatase fails to activate whole-cell TRPML1 currents. No detectable $I_{ML1\text{-}4A}$ was observed with or without Rapamycin (0.5 μM) application in ML1–4A –expressing HEK293 stable cells transfected with inactive mutant (D281A) of FKBP-5-phosphatase (FKBP-5-ptase-D281A) together with PM-FRB, which contains a signal for the PM localization. The dimerization of FRB and FKBP induced by rapamycin (0.5 μM for 10 min) led to translocation of 5-phosphatase from the cytosol to the PM. $I_{ML1\text{-}4A}$ was readily activated by SF-51 in the same cell.

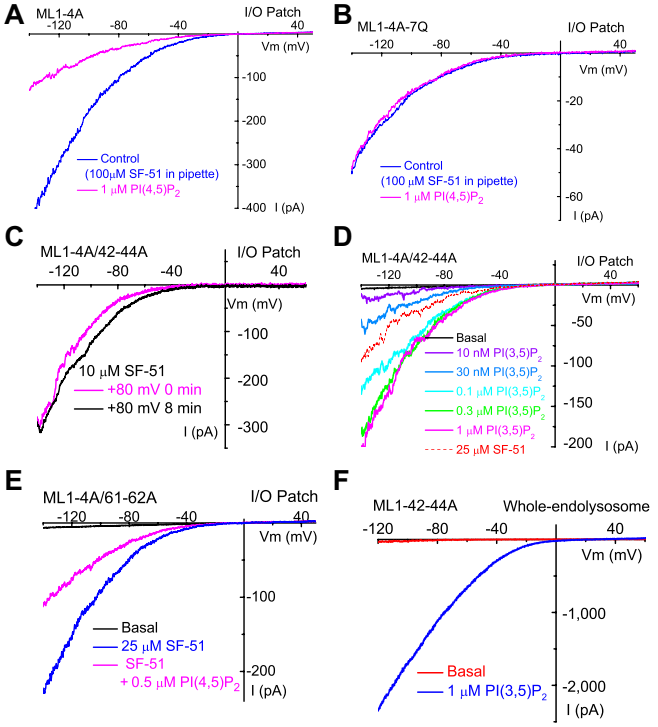

Fig. S8. Mutational analysis of $PI(4,5)P_2$ inhibition and $PI(3,5)P_2$ activation of TRPML1. (*A* and *B*) $PI(4,5)P_2$ inhibition is abolished by 7Q mutations in I/O patches. (*A*) Activation of $I_{ML1\text{-}4A}$ by SF-51 (100 μM; included in pipette solution) was significantly inhibited by bath application of $PI(4,5)P_2$ (1 μM). (*B*) Activation of $I_{ML1\text{-}4A\text{-}7Q}$ by SF-51 (100 μM; included in pipette solution) was insensitive to $PI(4,5)P_2$ (1 μM). (*C*) Triple mutations in the PIP_2-interacting domain abolish the activation effect of Ci-VSP. Activation of Ci-VSP by depolarization (HP = +80 mV) failed to potentiate the SF-51(10 μM)-activated $I_{ML1\text{-}4A/42\text{–}44A}$. (*D*) Dose-dependent activation of ML1–4A/42–44A by $PI(3,5)P_2$. $I_{ML1\text{-}4A/42\text{–}44A}$ was activated by various concentrations of $PI(3,5)P_2$ (10 nM, 30 nM, 0.1 μM, 0.3 μM, and 1 μM). Effect of SF-51 (25 μM) is shown for comparison. (*E*) $PI(4,5)P_2$ sensitivity of R61A/K62A double mutations. Activation of $I_{ML1\text{-}4A/61\text{–}62A}$ by SF-51 (25 μM) was inhibited by $PI(4,5)P_2$ (0.5 μM). (*F*) Activation of ML1-42–44A by $PI(3,5)P_2$ in the lysosome. Whole-endolysosome $I_{42\text{–}44A}$ was robustly activated by $PI(3,5)P_2$ (1 μM).